

# A MIXED SUSPENSION SYSTEM FOR A HALF-CAR VEHICLE MODEL

Alessandro Giua, Carla Seatzu, Giampaolo Usai,

Dip. di Ingegneria Elettrica ed Elettronica, Università di Cagliari,

Piazza d'Armi — 09123 Cagliari, Italy

Phone: +39-70-675.58.53 – Fax: +39-70-675.59.00 – Email: {giua,seatzu}@diee.unica.it.

## Abstract

*In this paper we realize the design of a mixed suspension system (an actuator in tandem with a conventional passive suspension) for the axle-tree of a road vehicle based on a linear model with four degrees of freedom. We propose an optimal control law that aims to optimize the suspension performance while ensuring that the magnitude of the forces generated by the two actuators and the total forces applied between wheel and body never exceed given bounds. The solution we derive takes the form of an adaptive control law that switches between different constant state feedback gains. The results of our simulations show that the bound on the active forces is a design parameter useful for establishing a trade-off between performance and power requirement.*

**Keywords:** active suspensions, mixed active–passive suspensions, LQR control, optimal gain switching.

Published as: A.Giua, C.Seatzu, G. Usai, "A Mixed Suspension System for a Half-Car Vehicle Model", *Dynamics and Control*, Vol. 10, No. 4, pp. 375–397, December 2000.

# 1 Introduction

The suspension system of most vehicles is purely *passive*, i.e., can be schematized as composed of passive elements, e.g., dampers and springs.

In an *active suspension* the interaction between vehicle body and wheel is regulated by an actuator of variable length. The actuator is usually hydraulically controlled and applies between body and wheel a force that represents the control action generally determined with an optimization procedure.

Active suspensions [3, 9, 16] have better performance than passive suspensions [2, 10]. However, the associated power, that must be provided by the vehicle engine, may reach the order of several 10 kW [7] depending on the required performance. As a viable alternative to a purely active suspension system, the use of *mixed active-passive suspensions* (an actuator in parallel with a passive suspension) has been considered [1, 5, 7, 8, 11, 14]. Such a system requires a lower power controller. Furthermore, even in case of malfunctioning of the active subsystem the vehicle needs not halt because the passive suspension can still function.

In this paper we first consider a linear mathematical model of the axletree suspension system schematized in figure 1. Then, we propose an optimal control law for tandem active-passive suspensions that aims to optimize the system performance while ensuring that the magnitude of the forces generated by the actuators never exceed a desired value  $u_{\max}$  and the magnitude of the total forces applied between wheel and body never exceed a desired value  $u_{T,\max}$ . The performance that can be taken into account with this model includes the decoupling between unsprung and sprung mass (the suspension aims to making the body of the vehicle less sensitive to the disturbances generated by the road profile acting on the wheel) and the minimization of the *rolling* behaviour. ....

This optimization problem takes the form:

$$\begin{aligned}
 \min J &= \sum_{k=0}^{\infty} \mathbf{x}^T(k) \mathbf{Q} \mathbf{x}(k) \\
 \text{s.t.} & \\
 (a) \quad & \mathbf{x}(k+1) = \mathbf{G} \mathbf{x}(k) + \mathbf{H} \mathbf{u}(k) \\
 (b) \quad & |u_i(k)| \leq u_{\max}, \quad i = 1, 2 \\
 (b') \quad & |u_i(k) - u_{pi}(k)| \leq u_{T,\max}, \quad i = 1, 2
 \end{aligned} \tag{1}$$

where  $\mathbf{x}$  is the system state,  $\mathbf{u}$  is a vector whose components are the control forces provided by the actuators,  $\mathbf{u}_p \equiv -\mathbf{k}_p \mathbf{x}$  is a vector whose components are the forces generated by the passive suspensions, and  $\mathbf{u}_T \equiv \mathbf{u} - \mathbf{k}_p \mathbf{x}$  is the vector of total forces. The optimal solution of this problem is denoted  $\mathbf{u}^*$ .

The performance of the suspension system is related to the minimization of the term  $\mathbf{x}^T \mathbf{Q} \mathbf{x}$ . The constraint (b) on the active forces limits the maximal force required from each controller, i.e., it leads to the choice of suitable actuators. The constraint (b') on the total forces bounds the acceleration of the sprung masses so as to ensure the comfort of passengers. Furthermore, this second constraint reduces the risk of loss of contact between wheel and road: in fact, the

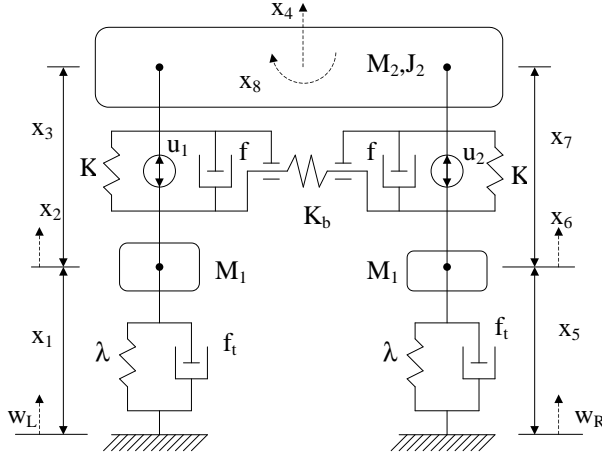


Figure 1: *Mixed suspension.*

loss of contact is possible when the sum of the total force  $u_T$  acting on the wheel and of its inertial force is directed upwards and has a magnitude greater than the weight resting on the wheel (that is not explicitly represented in the variation model we consider).

The main problem with this approach is that in general the law  $\mathbf{u}^*$  cannot be implemented as a feedback law with constant gains and it is difficult to compute [17]. Thus its implementation on on-board controllers is difficult at present time.

A valid solution to an optimization problem of the form (1) with only one constraint of the form (b) and with scalar input  $u$ , has been proposed by Yoshida *et al.* in [18, 19]. The proposed methodology consists in the approximation of the optimal law  $u^*$  by means of an adaptive controller that switches between different constant state feedback gains. Each  $\mathbf{k}_\varrho$  is the state feedback gain that gives the *unconstrained* optimal feedback law that minimizes a performance index of the form

$$J_\varrho = \sum_{k=0}^{\infty} \varrho \mathbf{x}^T(k) \mathbf{Q} \mathbf{x}(k) + r u^2(k)$$

where  $\varrho$  belongs to a discrete set. Yoshida provides a simple algorithm for choosing the suitable  $\varrho$  (i.e., suitable gains) as a function of the present system state while always ensuring that  $|u| \leq u_{\max}$  holds. When the system state is far from the origin a large  $\varrho$  (i.e., small gains) is selected, while for small disturbances a small  $\varrho$  (i.e., large gains) may be used. Yoshida's procedure can also ensure the stability of the gain-scheduled system: this is an important issue because in general stability of a system controlled by gain-scheduling is difficult to prove [15].

In this paper we show how Yoshida's procedure can be extended to more general optimization problems where the input is not necessarily a scalar entry and more than one constraint is present, each constraint being in general a linear combination of the input and of the state, as it is the case with constraint (b') of (1). We call the corresponding law *Optimal Gain Switching* (OGS) and denote it  $\mathbf{u}_{OGS}$ .

The results of the numerical simulations we have performed and that are discussed in Section 5

show that the optimal control laws  $\mathbf{u}^*$  and  $\mathbf{u}_{OGS}$  are very similar and the corresponding evolution of the suspension systems are almost identical. Thus the procedure we propose is a viable alternative to solve optimization problems of the form (1).

When compared with the LQR controller [1, 3, 14, 16], the OGS controller has two fundamental advantages. Firstly, it ensures a bound on the magnitude of the forces that each actuator needs to provide. As we impose more strict bounds on the magnitude of the active forces, we have worse performance in terms of sprung mass displacement. Thus, this bound can be seen as a design parameter to establish a trade-off between good performance and power requirement. Secondly, while LQR controllers realize a particular trade-off between performance (term  $\mathbf{x}^T Q \mathbf{x}$ ) and comfort (that depends on the total forces), the OGS controllers adapt the trade-off to different road conditions and car velocities, applying different control laws depending on the magnitude of the disturbance.

The need for adaptive suspensions is deeply felt in many applications such as Sport Utility Vehicles (SUV), a class of vehicles that is gaining more and more market shares both in USA and Europe. It is desirable that such a vehicle behaves as a normal car on-road, while offering the same performance of an off-road vehicle on a rough profile. The approach proposed in this paper answers to this need, because it leads to design a suspension that is not too soft for small disturbances, and not too stiff for large disturbances.

An OGS-based control law was also used in [6] to design a semi-active suspension system where the target law is approximated by controlling the damper coefficient of the suspension. In the present paper there are three main extensions with respect to [6]: an axle-tree model rather than a simpler quarter-car model; the use of a tandem suspension rather than a semi-active one; the generalization of the OGS procedure to multiple constraints on both inputs and state variables.

The paper is structured as follows. In Section 2 we recall the fundamental steps of the OGS procedure in the case of a single constraint which limits the magnitude of a linear combination of the input and of the state, and show how it can be extended to the solution of a more general problem with multiple constraints. In Section 3 we present the dynamical model of the suspension system. Section 4 shows how this procedure can be used to design a tandem active-passive suspension. Section 5 presents the results of some numerical simulations. In particular, we show how the bound on the active forces can be seen as a design parameter useful for establishing a trade-off between performance and power requirement. The results of a simulation where the road profile is taken into account as an external disturbance are also presented. Conclusions are drawn in Section 6. Finally, in the Appendix we have reported the algorithm used to compute the optimal law  $\mathbf{u}^*$  whose performance are considered as a reference for the  $\mathbf{u}_{OGS}$  law. This algorithm is the extension to the multiconstraint and vectorial input case of an algorithm by Yoshida [20].

## 2 Optimal Gain Switching Procedure

Let

$$\mathbf{x}(k+1) = \mathbf{G}\mathbf{x}(k) + \mathbf{H}\mathbf{u}(k) \quad (2)$$

be a linear time-invariant dynamic system, where  $\mathbf{x} \in \mathbb{R}^n$  is the system's state,  $\mathbf{u} \in \mathbb{R}^m$  is the system input,  $\mathbf{G} \in \mathbb{R}^{n \times n}$  and  $\mathbf{H} \in \mathbb{R}^{n \times m}$ .

Let us consider the following optimization problem:

$$\begin{aligned} \min J &= \sum_{k=0}^{\infty} \mathbf{x}^T(k) \mathbf{Q} \mathbf{x}(k), \\ \text{s.t.} & \\ (a) \quad & \mathbf{x}(k+1) = \mathbf{G}\mathbf{x}(k) + \mathbf{H}\mathbf{u}(k) \\ (b) \quad & |\boldsymbol{\alpha}_j^T \mathbf{u}(k) + \boldsymbol{\beta}_j^T \mathbf{x}(k)| \leq \gamma_j \quad k \geq 0, \quad j = 1, \dots, p, \end{aligned} \quad (3)$$

where  $\mathbf{Q}$  is positive semidefinite,  $\boldsymbol{\alpha}_j \in \mathbb{R}^m$  and  $\boldsymbol{\beta}_j \in \mathbb{R}^n$ . In this problem, in addition to constraint (a) that represents the system's dynamics, we have  $p$  constraints of the form (b): each one limits the magnitude of a linear combination of the input and of the state entries.

This optimal control problem has already been studied in the particular case of a scalar input and a single constraint ( $p = 1$ ) on the input magnitude ( $\alpha_1 = 1$ ,  $\beta_1 = \mathbf{0}$ ). In such a case the constraint takes the simpler form:

$$|u(k)| \leq \gamma \quad k \geq 0. \quad (4)$$

Wonham and Johnson [17] demonstrated that in this case the optimal solution  $u^*(\cdot)$  does not correspond in general to a feedback control law and furthermore, its computation is quite burdensome. Yoshida *et al.* [18] have proposed a simple procedure that approximates such optimal control law  $u^*(\cdot)$  by switching among feedback control laws whose gains can be computed solving a family of LQR problems.

In this paper we extend Yoshida's procedure to solve the more general problem (3). We call this procedure *Optimal Gain Switching* (OGS) and the corresponding feedback law will be denoted as  $\mathbf{u}_{\text{OGS}}(\cdot)$ .

### 2.1 Single constraint

Let us consider a linear time-invariant system of the form (2) and the corresponding optimization problem of the form (3) with a single constraint (b). Furthermore, let us consider a family of performance indexes  $J_\rho$  of the form

$$J_\rho = \sum_{k=0}^{\infty} \rho \mathbf{x}^T(k) \mathbf{Q} \mathbf{x}(k) + \mathbf{u}^T(k) \mathbf{R} \mathbf{u}(k). \quad (5)$$

For a given value of  $\varrho$  the *unconstrained* control law  $\mathbf{u}_\varrho(\cdot)$  that minimizes  $J_\varrho$  for system (2) can be written as

$$\mathbf{u}_\varrho(k) = -\mathbf{k}_\varrho \mathbf{x}(k) \quad (6)$$

where the gain matrix  $\mathbf{k}_\varrho$  can be computed by solving an algebraic Riccati equation [12]. Furthermore, for every gain factor  $\varrho$  it is possible to compute a *linear region*  $\Gamma_\varrho$  in the state space such that for any point  $\mathbf{x}_0$  within this region the following equation holds  $\forall k \geq 0$ :

$$|\boldsymbol{\alpha}^T \mathbf{u}_\varrho(k) + \boldsymbol{\beta}^T \mathbf{x}(k)| \equiv |(-\boldsymbol{\alpha}^T \mathbf{k}_\varrho + \boldsymbol{\beta}^T) \hat{\mathbf{G}}_\varrho^k \mathbf{x}_0| \leq \gamma \quad (7)$$

where  $\hat{\mathbf{G}}_\varrho = \mathbf{G} - \mathbf{H} \mathbf{k}_\varrho$ . Thus, if we consider the system (2) with control feedback law  $\mathbf{u}_\varrho$  and an initial state  $\mathbf{x}_0 \in \Gamma_\varrho$  we can be sure that in its future evolution the value of the control input and of the state are such that equation (3.b) is always satisfied.

The following proposition and constructive algorithm provide a simple procedure to determine if  $\mathbf{x}_0 \in \Gamma_\varrho$ . Proofs are omitted here because they are similar to those reported in [18] although we consider the case of a more general constraint of the form (3.b).

**Proposition 1.** Let  $\Gamma_\varrho$  be a linear region defined as above and  $\mathbf{x}_0$  a generic initial state vector. There exists a finite  $q_\varrho \in \mathbb{N}$  such that  $\mathbf{x}_0 \in \Gamma_\varrho$  iff equation (7) is satisfied for  $k = 0, 1, \dots, q_\varrho$ . ■

The value of  $q_\varrho$  can be easily computed. In fact, let us define for  $k \in \mathbb{N}$  the sequence of vectors  $\mathbf{z}_k^T = (-\boldsymbol{\alpha}^T \mathbf{k}_\varrho + \boldsymbol{\beta}^T) \hat{\mathbf{G}}_\varrho^k$  and let

$$\mathcal{C}(\mathbf{z}_0, \dots, \mathbf{z}_q) := \{\mathbf{z} = a_0 \mathbf{z}_0 + \dots + a_q \mathbf{z}_q \mid |a_0| + \dots + |a_q| \leq 1\}$$

be the set of convex combinations of the vectors  $\pm \mathbf{z}_0, \dots, \pm \mathbf{z}_q$ .

In [18] it was proved that  $q_\varrho$  is the smallest non negative integer such that  $\mathbf{z}_{q_\varrho+1} \in \mathcal{C}(\mathbf{z}_0, \dots, \mathbf{z}_{q_\varrho})$ . Furthermore, to check if a vector  $\mathbf{z}$  belongs to  $\mathcal{C}(\mathbf{z}_0, \dots, \mathbf{z}_q)$  we may compute the  $n \times (2q + 2)$  matrix  $\mathbf{D} := [\hat{\mathbf{z}}_0, \hat{\mathbf{z}}_1, \dots, \hat{\mathbf{z}}_{2q+1}]$  where

$$\begin{cases} \hat{\mathbf{z}}_i := \mathbf{z}_i - \mathbf{z}, \\ \hat{\mathbf{z}}_{i+q+1} := -\mathbf{z}_i - \mathbf{z}, \end{cases} \quad i = 0, \dots, q$$

and solve the following linear programming problem (LPP) where we have denoted  $\mathbf{1}$  a vector of 1's

$$\begin{aligned} & \max \mathbf{1}^T \mathbf{y} \\ & \text{s.t.} \\ & \begin{cases} \mathbf{D} \mathbf{y} = 0 \\ \mathbf{y} \geq 0. \end{cases} \end{aligned}$$

The vector  $\mathbf{z}$  belongs to  $\mathcal{C}(\mathbf{z}_0, \dots, \mathbf{z}_q)$  iff the optimal solution of this LPP is unbounded.

Thus, having computed the value of  $q_\varrho$ , if we choose

$$\mathbf{Z}_\varrho = \frac{1}{\gamma} \begin{bmatrix} \mathbf{z}_0^T \\ \mathbf{z}_1^T \\ \vdots \\ \mathbf{z}_{q_\varrho}^T \end{bmatrix}.$$

we have that  $\mathbf{x}_0 \in \Gamma_\varrho$  if and only if

$$-\mathbf{1} \leq \mathbf{Z}_\varrho \mathbf{x}_0 \leq \mathbf{1}.$$

The control procedure can be briefly summarized as follows. A set of LQ optimal feedback gains corresponding to different weighting factors in the quadratic function  $J_\varrho$  is chosen, and then, at each sampling instant, the highest gain  $\varrho$  such that the current state  $\mathbf{x}(k)$  belongs to  $\Gamma_\varrho$  is applied. Note that in Yoshida's approach the switching of gains leads to a monotonically nondecreasing sequence of  $\varrho$  if we assume no external disturbance is acting on the system. This is the essential feature of the method and allows us to extend to the OGS law the stability property enjoyed by LQR control laws, while reducing the performance index  $\sum_{k=0}^{\infty} \mathbf{x}(k)^T \mathbf{Q} \mathbf{x}(k)$  with respect to a fixed gain.

A final comment regarding the OGS procedure. Each gain matrix is computed for an infinite time horizon solving an algebraic Riccati equation, but is used only for a finite time horizon (with the exception of the gain matrix corresponding to the highest  $\varrho$ ). The idea of computing the OGS gains for a finite horizon (solving a dynamic Riccati equation) is not practical, because the switching times are not easy to compute and this law would lead to time-varying gains.

## 2.2 Multiple constraints

Now, let us consider the multiple constraint optimization problem of the form (3). In such a case the same discussion as above can be repeated for every constraint. So we can define:

$$\mathbf{Z}_\varrho = \begin{bmatrix} \mathbf{Z}_{\varrho,1} \\ \mathbf{Z}_{\varrho,2} \\ \vdots \\ \mathbf{Z}_{\varrho,p} \end{bmatrix}, \quad \mathbf{Z}_{\varrho,j} = \frac{1}{\gamma_j} \begin{bmatrix} -\boldsymbol{\alpha}_j^T \mathbf{k}_\varrho + \boldsymbol{\beta}_j^T \\ (-\boldsymbol{\alpha}_j^T \mathbf{k}_\varrho + \boldsymbol{\beta}_j^T) \hat{\mathbf{G}}_\varrho \\ \vdots \\ (-\boldsymbol{\alpha}_j^T \mathbf{k}_\varrho + \boldsymbol{\beta}_j^T) \hat{\mathbf{G}}_\varrho^{q_{e,j}} \end{bmatrix},$$

where each matrix  $\mathbf{Z}_{\varrho,j}$  is relative to the  $j$ -th constraint of type (3.b). Note, however, that in general the matrix  $\mathbf{Z}_\varrho$  may have redundant rows (i.e., rows that belong to the convex combination of the other ones) and that can be determined solving an LPP as outlined above. We discard the redundant rows thus obtaining a matrix of  $\tilde{q}$  rows that we call  $\tilde{\mathbf{Z}}_\varrho$ . As in the single constraint problem we have that

$$-\mathbf{1} \leq \tilde{\mathbf{Z}}_\varrho \mathbf{x}_0 \leq \mathbf{1} \quad \Leftrightarrow \quad \mathbf{x}_0 \in \bigcap_{j=1}^p \Gamma_{\varrho,j}.$$

We propose to choose, at each sampling instant, the highest gain  $\varrho$  from a given finite set, such that the current state  $\mathbf{x}$  belongs to  $\Gamma_\varrho = \bigcap_{j=1}^p \Gamma_{\varrho,j}$ . Therefore, the control procedure consists in two phases and can be briefly summarized with the following algorithm.

**Algorithm 2.** *Optimal Gain Switching (OGS).* The algorithm is divided into off-line and on-line portions.

*Off-line phase*

1. Choose a finite set of  $r$  values for  $\varrho$ , namely  $\{\varrho_1, \varrho_2, \dots, \varrho_r\}$ , with  $\varrho_1 < \varrho_2 < \dots < \varrho_r$ .
2. Determine for each  $\varrho_i$  the corresponding gain matrix  $\mathbf{k}_{\varrho_i}$  by solving an LQR problem with performance index of the form (5).
3. Construct for each  $\varrho_i$  the corresponding matrix  $\tilde{\mathbf{Z}}_{\varrho_i}$ , following the procedure described above.

*On-line phase*

1. Let  $k := 0$ .
2. Let  $\bar{\varrho} := \max_i \{\varrho_i \mid \mathbf{x}(k) \in \bigcap_{j=1}^p \Gamma_{\varrho_i, j}\}$ .
3. Set up the control according to  $\mathbf{u}(k) = -\mathbf{k}_{\bar{\varrho}} \mathbf{x}(k)$ .
4. Put  $k := k + 1$  and return to Step 2. ■

If the initial state  $\mathbf{x}(0) \in \Gamma_{\varrho}$  for  $\varrho \in \{\varrho_1, \dots, \varrho_r\}$ , then we can be sure that, in the absence of external disturbances, at Step 3 of the on-line phase a value  $\bar{\varrho}$  always exists. In fact, the value of  $\bar{\varrho}$  determined at the previous iteration can still be used if a higher value cannot be found. Thus we can be sure that in the absence of external disturbances the switching of feedback gains leads to a monotonically nondecreasing value of  $\varrho$ , so stability is ensured.

It is important to highlight the advantages and limits of the OGS control scheme. It has been shown by Yoshida, in the case of a single constraint of the form (4), that the control law  $\mathbf{u}_{\text{OGS}}(\cdot)$  leads to values of the performance index in (3) that are close to the absolute minimum given by the optimal control law  $\mathbf{u}^*(\cdot)$ . In the following we will show, by numerical simulations, that the same conclusions are still valid in presence of multiple constraints.

The computational complexity of the OGS control law warrants comment. The most burdensome part of this procedure is the off-line phase, where the matrices  $\mathbf{Z}_{\varrho, j}$  are computed. During the on-line phase, it is necessary to compute at most  $r \times p$  matrix products  $\mathbf{Z}_{\varrho_i, j} \mathbf{x}(k)$  at each sampling instant  $k$ . The number of rows of the different  $\mathbf{Z}_{\varrho_i, j}$  is not constant and is equal to  $q_{\varrho_i, j} + 1$ . In Section 5, we will discuss the computational complexity relative to the determination of the OGS control law.

### 3 Dynamical model of the suspension system

We refer to the completely active suspension with four degrees of freedom schematized in figure 2. We used the following notation:

- $M_1$  is the equivalent unsprung mass of the wheel and of the moving parts of the suspension connected thereto;

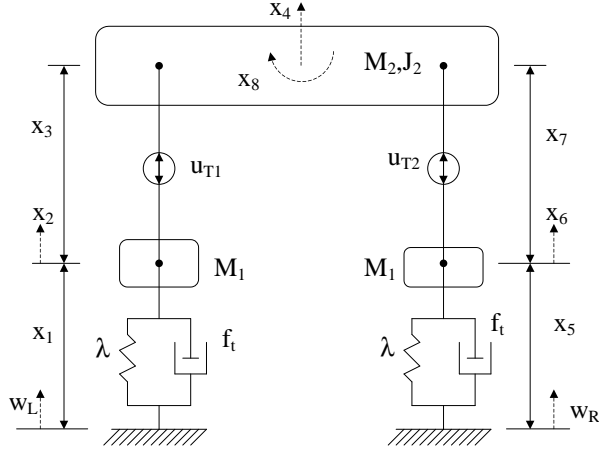


Figure 2: *Active suspension.*

- $M_2$  is the sprung mass, i.e., the part of the whole body mass and the load mass pertaining to the axletree;
- $J_2$  is the moment of inertia of the sprung mass with respect to the barycentric axis perpendicular to the drawing plane;
- $\lambda$  is the elastic constant of the tire;
- $f_t$  is the coefficient that takes into account the damping of the tire;
- $2d$  is the wheel-track;
- $x_1(t)$ ,  $x_3(t)$ ,  $x_5(t)$ ,  $x_7(t)$  represent the deformations with respect to the static equilibrium configuration, taken as positive if they are elongations, of the left tire, left suspension, right tire and right suspension, respectively;
- $x_2(t)$ ,  $x_6(t)$ ,  $x_4(t)$  represent the absolute vertical velocities, taken as positive if directed upwards, of the barycentres of the unsprung left and right-hand mass and sprung mass respectively;
- $x_8(t)$  represents the angular velocity, taken as positive when clockwise, of the sprung mass;
- $u_{T1}$ ,  $u_{T2}$  represent the left and right total control forces respectively.

The above system can be modeled with the following equation

$$\dot{\mathbf{x}}(t) = \mathbf{A}\mathbf{x}(t) + \mathbf{B}\mathbf{u}_T(t) \quad (8)$$

where  $\mathbf{x}(t) \in \mathbb{R}^8$  is the state,  $\mathbf{u}_T(t) \in \mathbb{R}^2$  is the control input,  $\mathbf{A} \in \mathbb{R}^{8 \times 8}$  and  $\mathbf{B} \in \mathbb{R}^{8 \times 2}$  are constant matrices with the following structure:

$$\mathbf{A} = \begin{bmatrix} 0 & 1 & 0 & 0 & 0 & 0 & 0 & 0 \\ -\frac{\lambda}{M_1} & -\frac{f_t}{M_1} & 0 & 0 & 0 & 0 & 0 & 0 \\ 0 & -1 & 0 & 1 & 0 & 0 & 0 & d \\ 0 & 0 & 0 & 0 & 0 & 0 & 0 & 0 \\ 0 & 0 & 0 & 0 & 0 & 1 & 0 & 0 \\ 0 & 0 & 0 & 0 & -\frac{\lambda}{M_1} & -\frac{f_t}{M_1} & 0 & 0 \\ 0 & 0 & 0 & 1 & 0 & -1 & 0 & -d \\ 0 & 0 & 0 & 0 & 0 & 0 & 0 & 0 \end{bmatrix}, \quad \mathbf{B} = \begin{bmatrix} 0 & 0 \\ -\frac{1}{M_1} & 0 \\ 0 & 0 \\ \frac{1}{M_2} & \frac{1}{M_1} \\ 0 & 0 \\ 0 & -\frac{1}{M_1} \\ 0 & 0 \\ \frac{d}{J_2} & -\frac{d}{J_2} \end{bmatrix}.$$

## 4 Design of a tandem active-passive suspension

A completely active suspension comprises numerous parts, where the main component is an actuator that is capable of supplying the entire control force, and its dimension satisfies the system's maximum power requirements. We examine the possibility of reducing the power requirements, and hence the size of the active part of the suspensions, using a combination of active and passive components as shown in figure 1, where the passive components are assigned the task of providing part of the control actions thereby minimizing the power absorbed by the active part.

The following notation has been used in the figure:

- $K$  is the elastic constant of the spring;
- $f$  is the characteristic coefficient of the damper;
- $K_b$  is the elastic constant of the stabilizing bar;
- $\mathbf{u} = [u_1, u_2]^T$  is the vector of control forces that must be realized by the actuators.

The passive components are assumed to exhibit linear behaviour.

It is easily shown that the passive suspension provides a contribution  $\mathbf{u}_p(t)$  to the total control forces  $\mathbf{u}_T(t)$  which can be expressed as:

$$\mathbf{u}_p(t) = -\mathbf{k}_p \mathbf{x}(t) \quad (9)$$

being:

$$\mathbf{k}_p = \begin{bmatrix} 0 & -f & (K + K_b) & f & 0 & 0 & -K_b & d \cdot f \\ 0 & 0 & -K_b & f & 0 & -f & (K + K_b) & -d \cdot f \end{bmatrix}. \quad (10)$$

So, at every instant, it is:

$$\mathbf{u}_T(t) = \mathbf{u}_p(t) + \mathbf{u}(t). \quad (11)$$

Let us observe the dynamical system schematized in figure 1 and described by equation (8). It can also be thought of as a system with only the active control input and a different dynamical matrix, so equation (8) can be rewritten as:

$$\dot{\mathbf{x}}(t) = (\mathbf{A} - \mathbf{B}\mathbf{k}_p)\mathbf{x}(t) + \mathbf{B}\mathbf{u}(t) = \mathbf{A}_p\mathbf{x}(t) + \mathbf{B}\mathbf{u}(t). \quad (12)$$

Note that the control law we will design in the following sections requires the knowledge of the system state, that is not directly measurable. However it can be reconstructed through an appropriate state observer, assuming available the measurements of the suspension deformations and the sprung mass velocity (via an accelerometer) [6].

The control approach we will follow uses a discrete-time state space model. Thus we choose a sampling interval  $T$  and discretize equation (12) to obtain

$$\mathbf{x}(k+1) = \mathbf{G}_p\mathbf{x}(k) + \mathbf{H}\mathbf{u}(k) \quad (13)$$

where

$$\mathbf{G}_p = e^{\mathbf{A}_p T}, \quad \mathbf{H} = \left( \int_0^T e^{\mathbf{A}_p \tau} d\tau \right) \mathbf{B}.$$

It is known [13] that a system that is stabilizable and observable in the absence of sampling maintains these properties after the introduction of sampling if and only if, for every eigenvalue of the characteristic equation for the continuous-time control system, the relationship

$$Re\{\lambda_i\} = Re\{\lambda_j\} \quad (14)$$

implies that

$$Im\{\lambda_i - \lambda_j\} \neq \frac{2n\pi}{T} \quad n = \pm 1, \pm 2, \dots \quad (15)$$

is satisfied.

Now, let us consider a family of performance indexes:

$$J_\rho = \sum_{k=0}^{\infty} \rho \mathbf{x}^T(k) \mathbf{Q} \mathbf{x}(k) + \mathbf{u}(k) \mathbf{R} \mathbf{u}(k). \quad (16)$$

We want to apply the OGS procedure to system (13) and determine the corresponding feedback control law such that the following constraints hold:

$$|u_i(k)| \leq u_{\max}, \quad i = 1, 2, \quad (17)$$

$$|u_{T_i}(k)| \leq u_{T, \max}, \quad i = 1, 2. \quad (18)$$

This means that we can determine a control law whose magnitude is bounded in order to reach a good trade-off between road holding and comfort of passengers. Under appropriate assumptions

on the maximum value of the suspension deformation velocity, the bound on the active control forces allows us to constrain the power supplied by the actuators and can be used to design each actuator in terms of the required power. Constraints (17) and (18) are of the form (3.b) with  $\boldsymbol{\alpha}_1 = \mathbf{e}_1$ ,  $\boldsymbol{\beta}_1 = \mathbf{0}$ ,  $\gamma_1 = u_{\max}$ ,  $\boldsymbol{\alpha}_2 = \mathbf{e}_2$ ,  $\boldsymbol{\beta}_2 = \mathbf{0}$ ,  $\gamma_2 = u_{\max}$ ,  $\boldsymbol{\alpha}_3 = \mathbf{e}_1$ ,  $\boldsymbol{\beta}_3^T = -\mathbf{e}_1^T \mathbf{k}_p$ ,  $\gamma_3 = u_{T,\max}$  and  $\boldsymbol{\alpha}_4 = \mathbf{e}_2$ ,  $\boldsymbol{\beta}_4^T = -\mathbf{e}_2^T \mathbf{k}_p$ ,  $\gamma_4 = u_{T,\max}$ , respectively, being  $\mathbf{e}_i$  the  $i$ -th column of the 2nd order identity matrix.

So we have:

$$\mathbf{Z}_{\rho,1} = \begin{bmatrix} -\mathbf{e}_1^T \mathbf{k}_\rho \\ -\mathbf{e}_1^T \mathbf{k}_\rho \hat{\mathbf{G}}_\rho \\ \vdots \\ -\mathbf{e}_1^T \mathbf{k}_\rho \hat{\mathbf{G}}_\rho^{q_{\rho,1}} \end{bmatrix}, \quad \mathbf{Z}_{\rho,2} = \begin{bmatrix} -\mathbf{e}_2^T \mathbf{k}_\rho \\ -\mathbf{e}_2^T \mathbf{k}_\rho \hat{\mathbf{G}}_\rho \\ \vdots \\ -\mathbf{e}_2^T \mathbf{k}_\rho \hat{\mathbf{G}}_\rho^{q_{\rho,2}} \end{bmatrix},$$

$$\mathbf{Z}_{\rho,3} = \begin{bmatrix} -\mathbf{e}_1^T (\mathbf{k}_\rho + \mathbf{k}_p) \\ -\mathbf{e}_1^T (\mathbf{k}_\rho + \mathbf{k}_p) \hat{\mathbf{G}}_\rho \\ \vdots \\ -\mathbf{e}_1^T (\mathbf{k}_\rho + \mathbf{k}_p) \hat{\mathbf{G}}_\rho^{q_{\rho,3}} \end{bmatrix}, \quad \mathbf{Z}_{\rho,4} = \begin{bmatrix} -\mathbf{e}_2^T (\mathbf{k}_\rho + \mathbf{k}_p) \\ -\mathbf{e}_2^T (\mathbf{k}_\rho + \mathbf{k}_p) \hat{\mathbf{G}}_\rho \\ \vdots \\ -\mathbf{e}_2^T (\mathbf{k}_\rho + \mathbf{k}_p) \hat{\mathbf{G}}_\rho^{q_{\rho,4}} \end{bmatrix}.$$

where  $\hat{\mathbf{G}}_\rho = \mathbf{G}_p - \mathbf{k}_\rho \mathbf{H}$ .

## 5 Application example

In this section we discuss the results of some numerical simulations.

The proposed procedure has been applied to the half-car vehicle model shown in figure 1, with values of the parameters taken from [4]:

- $M_1 = 28.58\text{Kg}$ ,
- $M_2 = 2 \times 288.90\text{Kg} = 577.8\text{Kg}$ ,
- $\lambda = 155900\text{N/m}$ ,
- $f_t = 400\text{Ns/m}$ ,
- $J_2 = 108.3\text{Kg m}^2$
- $d = 0.75\text{m}$ .

Furthermore, matrices  $\mathbf{Q}$  and  $\mathbf{R}$  have been chosen with the following structure [4]:

$$\mathbf{Q} = \begin{bmatrix} q_1 & 0 & 0 & 0 & 0 & 0 & 0 & 0 \\ 0 & 0 & 0 & 0 & 0 & 0 & 0 & 0 \\ 0 & 0 & q_2 + q_3 & 0 & 0 & 0 & -q_3 & 0 \\ 0 & 0 & 0 & 0 & 0 & 0 & 0 & 0 \\ 0 & 0 & 0 & 0 & q_1 & 0 & 0 & 0 \\ 0 & 0 & 0 & 0 & 0 & 0 & 0 & 0 \\ 0 & 0 & -q_3 & 0 & 0 & 0 & q_2 + q_3 & 0 \\ 0 & 0 & 0 & 0 & 0 & 0 & 0 & 0 \end{bmatrix}, \quad \mathbf{R} = \begin{bmatrix} r_1 & 0 \\ 0 & r_2 \end{bmatrix}$$

where  $q_1 = 10$ ,  $q_2 = 1$ ,  $q_3 = 0.5$ ,  $r_1 = r_2 = 0.8 \cdot 10^{-9}$ .

The values of the weights  $q_1$  (which penalizes the deformation of the tire),  $q_2$  (which penalizes the deformation of the suspension),  $q_3$  (which penalizes the sprung mass rotation),  $r_1$  and  $r_2$  (which penalize the forces supplied by the actuators), have been chosen following [4].

The values of

- $f = 1081\text{Ns/m}$ ,
- $K = 15438\text{N/m}$ ,
- $K_b = 5496\text{N/m}$

have been also taken from [4] where it was shown that this choice in nominal conditions maximizes the power associated with the control action of the passive part, thereby minimizing that required by the active part of the suspension.

The control approach we have followed in this paper makes use of a discrete-time state space model. A suitable choice of the sampling interval is  $T = 0.01\text{s}$  as discussed in [6].

We have taken  $u_{T,max} = 3000\text{N}$  that is slightly less than the total weight resting on one wheel. A higher total control force may cause the loss of contact between wheel and road. Furthermore, this constraint also limits the acceleration of the sprung mass and this is a necessary condition for the comfort of passengers.

Another important aspect of the proposed design procedure deals with the choice of the weighting coefficients  $\{\varrho_1, \varrho_2, \dots, \varrho_r\}$ . The weighting coefficient  $\varrho_1$  should be determined so that the linear region  $\Gamma_{\varrho_1,1} \cap \Gamma_{\varrho_1,2} \cap \Gamma_{\varrho_1,3} \cap \Gamma_{\varrho_1,4}$  contains all initial conditions of interest. The weighting coefficient  $\varrho_r$  should be selected so that the region  $\Gamma_{\varrho_r,1} \cap \Gamma_{\varrho_r,2} \cap \Gamma_{\varrho_r,3} \cap \Gamma_{\varrho_r,4}$  covers small disturbances or very little system noises. The other weighting coefficients have been chosen, following Yoshida [18], so that the ratio of the 2-norm for two adjacent total gains ( $\mathbf{k}_{\varrho_i} + \mathbf{k}_p$ ) is  $\simeq 1.6 \div 1.8$ . We have assumed  $r = 10$  as it seems a good trade-off between computational efficiency and performance index. The chosen values are shown in the table below. It can be noted that in this case  $q_{\varrho,1,\dots,4}$  are equal and are nonincreasing functions of  $\varrho$ .

$i$	1	2	3	4	5	6	7	8	9	10
$\varrho_i$	0.01	0.1	0.5	1	4	20	50	100	1000	$10^5$
$q_{\varrho_i,1}$	53	51	44	40	36	33	32	32	31	31
$q_{\varrho_i,2}$	53	51	44	40	36	33	32	32	31	31
$q_{\varrho_i,3}$	53	51	44	40	36	33	32	32	31	31
$q_{\varrho_i,4}$	53	51	44	40	36	33	32	32	31	31
$\sum_{j=1}^4 q_{\rho_i,j}$	212	204	176	160	144	132	128	128	124	124
$\tilde{q}_i$	113	96	79	65	53	49	47	47	46	47

In the last line of the table we have reported the values of  $\tilde{q}_i$ 's. Each  $\tilde{q}_i$ , as discussed in subsection 2.2, denotes the number of rows of  $\tilde{\mathbf{Z}}_{\rho_i}$ , obtained by  $\mathbf{Z}_{\rho_i}$  after deleting all redundant rows. As it can be seen, for each convex region, the number of independent constraints is about one half of the total number. Computing  $\tilde{\mathbf{Z}}_{\rho_i}$  increases the computational efforts when solving the off-line phase, but greatly improve the on-line phase, thus enabling us to compute the control law much more efficiently.

To evaluate the performance of the  $\mathbf{u}_{OGS}$  law, we compare it with the optimal law  $\mathbf{u}^*$ . The algorithm to compute the optimal law  $\mathbf{u}^*$  is the extension to the multiconstraint case of an algorithm by Yoshida [20] and consists in a sort of predictive control strategy whose application to real cases is not feasible because it provides a feedforward control law. The law  $\mathbf{u}^*$  has also been called *Perfect Optimal Control* (POC) and, in accordance with the literature, we denote it  $\mathbf{u}_{POC}$  in the rest of the section. This procedure can be briefly summarized with the algorithm reported in Appendix, that requires solving at each step several quadratic programming problems. The POC control law is not a function of the actual state, thus producing a feedforward control law. Therefore, while OGS control can be given as a set of predetermined gains, at each step the POC needs to be computed for an infinite time horizon. Such a difference become greatly relevant when external disturbances occur and POC needs to be recomputed at each sampling instant.

In our applicative case we have assumed  $\varrho_\infty = \varrho_{10}$  as we have observed that any increment in the gain factor with respect to  $\varrho_{10}$  corresponds to a negligible variation in the feedback control law. This fact can be explained considering that we are dealing with a discrete-time system.

In the following we provide the results of three series of numerical simulations in order to underline the main conclusions relative to the proposed procedure. In the first two simulations we assume that no external disturbance is acting on the system, while the initial state is different from zero; on the contrary, in the third simulation we assume that the system starts from the origin, but an external disturbance, representative of a very rough road profile, is acting on the system.

## 5.1 Simulation 1

In the first simulation we compare the performances of the system designed with OGS and POC procedures, and the system designed with conventional LQR technique.

We have considered  $u_{\max} = 600\text{N}$  and  $x_1(0) = -x_5(0) = 0.02\text{m}$ ,  $x_3(0) = -x_7(0) = 0.1\text{m}$ ,  $x_2(0) = x_4(0) = x_6(0) = 0\text{m/s}$ ,  $x_8(0) = 0\text{rad/s}$ . The results of simulations are reported in figures 3–4–5. In figures 3.a–d a comparison between the deformation of the suspensions and of the tires with OGS and POC control laws is presented. The rolling behaviour is given in figure 3.e that shows the angular position  $\theta$  of the sprung mass, taken as positive when clockwise, i.e.,  $\theta = \text{atg}((x_1 + x_3 - x_5 - x_7)/2d)$ . From these figures it is evident how close the evolutions of the two designed systems are. Figures 4.a–d show the evolution of the OGS and POC active and total control forces. Figure 5 shows the values of the index  $i$  of the linear regions  $\Gamma_{\rho_i,1}$ ,  $\Gamma_{\rho_i,2}$ ,  $\Gamma_{\rho_i,3}$  and  $\Gamma_{\rho_i,4}$ . Clearly the value of the index  $i$  relative to the region  $\Gamma_{\rho_i,1} \cap \Gamma_{\rho_i,2} \cap \Gamma_{\rho_i,3} \cap \Gamma_{\rho_i,4}$  is the minimum of the four indexes. We also observe that as the state approaches the origin the index  $i$  remains constant.

In figures 3–4 we also present a comparison with two mixed suspensions whose active part has been designed with the conventional LQR approach: the one for a value of  $\rho = \rho_1 = 0.01$  and the one for a value of  $\rho = \rho_4 = 1$ . As it can be seen, in the case of  $\rho_1$ , small forces are required from the actuators, but a long transient behaviour occurs. On the contrary, in the case of  $\rho_4$  the results, both in terms of tire and suspension deformations, and in terms of sprung mass rotation, are comparable to that obtained with the OGS control law, but with much larger forces magnitude.

A further numerical comparison among the above described control laws is given in the table below. In the first row we have reported  $\sum_k \mathbf{x}^T(k) \mathbf{Q} \mathbf{x}(k)$  and  $\sum_k \mathbf{u}^T(k) \mathbf{R} \mathbf{u}(k)$ . The third row shows the maximum value of the force required by the actuators. The last three lines provide the root mean square (rms) value of the sprung masses accelerations, and the rms values of the tires and suspensions deformations, respectively. This clearly highlight how the OGS-based controller provides a good compromise between performance and power requirement.

	CGO	POC	LQ ( $\rho_1$ )	LQ ( $\rho_4$ )
$\sum_{k=1}^{100} \mathbf{x}^T(k) \mathbf{Q} \mathbf{x}(k)$	$3.48 \cdot 10^{-1}$	$3.23 \cdot 10^{-1}$	$3.74 \cdot 10^{-1}$	$3.04 \cdot 10^{-1}$
$\sum_{k=1}^{100} \mathbf{u}^T(k) \mathbf{R} \mathbf{u}(k)$	$6.30 \cdot 10^{-3}$	$1.37 \cdot 10^{-2}$	$7.24 \cdot 10^{-4}$	$2.01 \cdot 10^{-2}$
$\max_{k=1, \dots, 100} u_1(k) = \max_{k=1, \dots, 100} u_2(k)$	584	600	193	1880
$\text{rms}(\dot{x}_2) = \text{rms}(\dot{x}_6)$	$5.47 \cdot 10^{-14}$	$5.64 \cdot 10^{-14}$	$3.02 \cdot 10^{-14}$	$3.31 \cdot 10^{-14}$
$\text{rms}(x_1) = \text{rms}(x_5)$	$5.05 \cdot 10^{-4}$	$5.17 \cdot 10^{-4}$	$4.92 \cdot 10^{-4}$	$5.51 \cdot 10^{-4}$
$\text{rms}(x_3) = \text{rms}(x_7)$	$2.71 \cdot 10^{-3}$	$2.60 \cdot 10^{-3}$	$2.90 \cdot 10^{-3}$	$2.50 \cdot 10^{-3}$

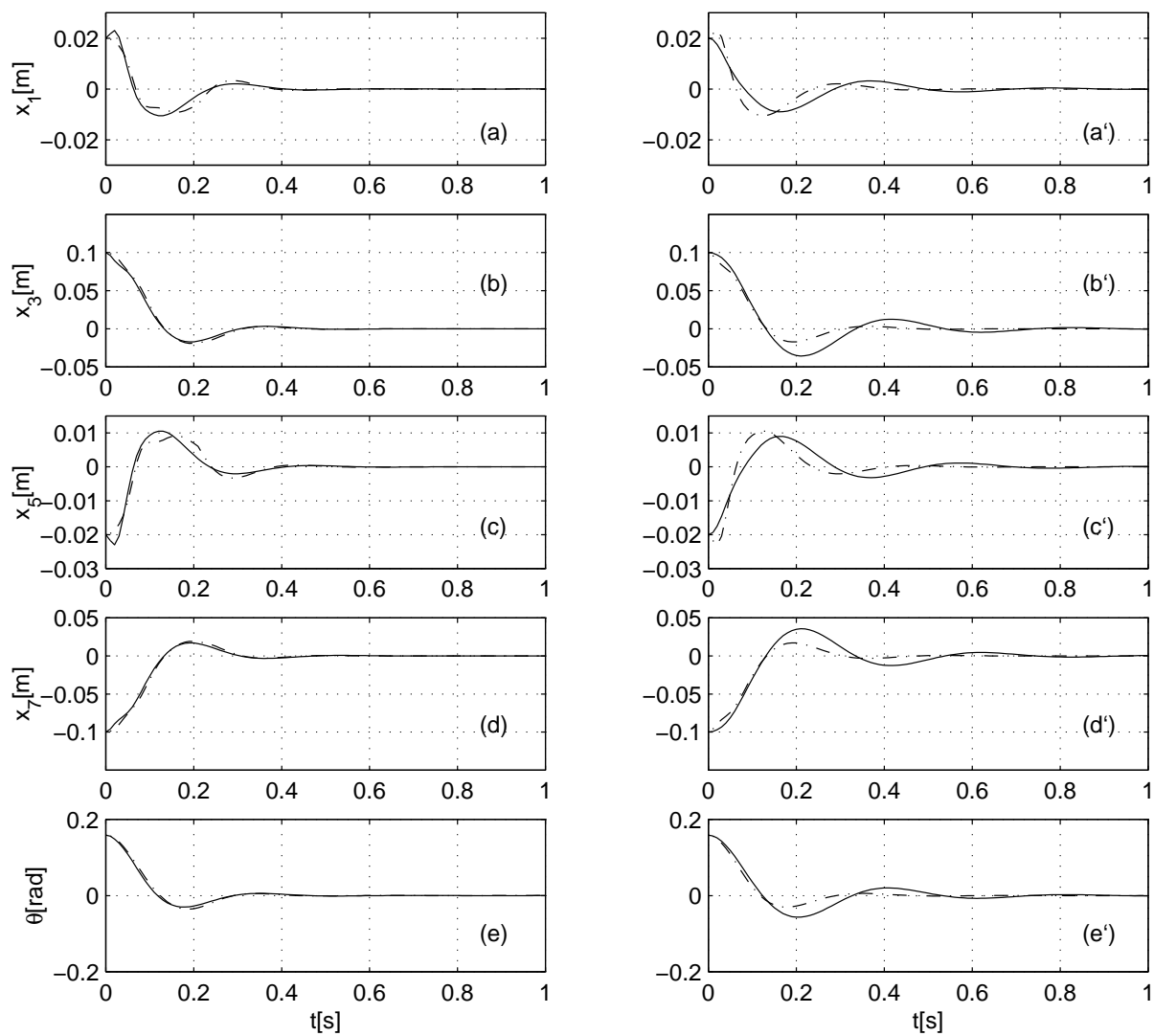


Figure 3: The results of simulation 1. (a) Evolution of  $x_{1,POC}$  (dotted) and  $x_{1,OGS}$  (continuous). (a') Evolution of  $x_{1,\rho_4}$  (dotted) and  $x_{1,\rho_1}$  (continuous). (b) Evolution of  $x_{3,POC}$  (dotted) and  $x_{3,OGS}$  (continuous). (b') Evolution of  $x_{3,\rho_4}$  (dotted) and  $x_{3,\rho_1}$  (continuous). (c) Evolution of  $x_{5,POC}$  (dotted) and  $x_{5,OGS}$  (continuous). (c') Evolution of  $x_{5,\rho_4}$  (dotted) and  $x_{5,\rho_1}$  (continuous). (d) Evolution of  $x_{7,POC}$  (dotted) and  $x_{7,OGS}$  (continuous). (d') Evolution of  $x_{7,\rho_4}$  (dotted) and  $x_{7,\rho_1}$  (continuous). (e) Evolution of  $\theta_{POC}$  (dotted) and  $\theta_{OGS}$  (continuous). (e') Evolution of  $\theta_{\rho_4}$  (dotted) and  $\theta_{\rho_1}$  (continuous).

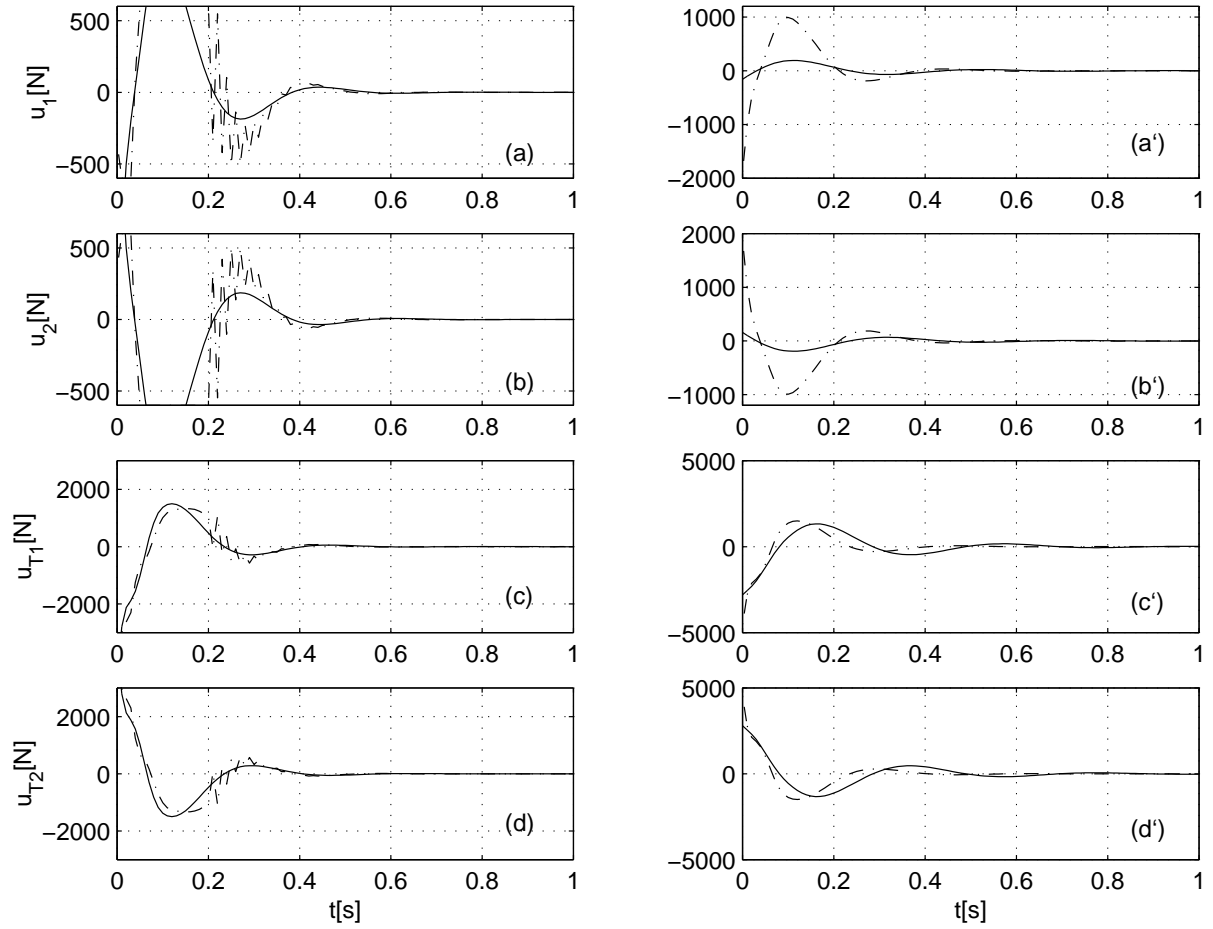


Figure 4: The results of simulation 1. (a) Evolution of  $u_{1,POC}$  (dotted) and  $u_{1,OGS}$  (continuous). (a') Evolution of  $u_{1,\rho_4}$  (dotted) and  $u_{1,\rho_1}$  (continuous). (b) Evolution of  $u_{2,POC}$  (dotted) and  $u_{2,OGS}$  (continuous). (b') Evolution of  $u_{2,\rho_4}$  (dotted) and  $u_{2,\rho_1}$  (continuous). (c) Evolution of  $u_{T1,POC}$  (dotted) and  $u_{T1,OGS}$  (continuous). (c') Evolution of  $u_{T1,\rho_4}$  (dotted) and  $u_{T1,\rho_1}$  (continuous). (d) Evolution of  $u_{T2,POC}$  (dotted) and  $u_{T2,OGS}$  (continuous). (d') Evolution of  $u_{T2,\rho_4}$  (dotted) and  $u_{T2,\rho_1}$  (continuous).

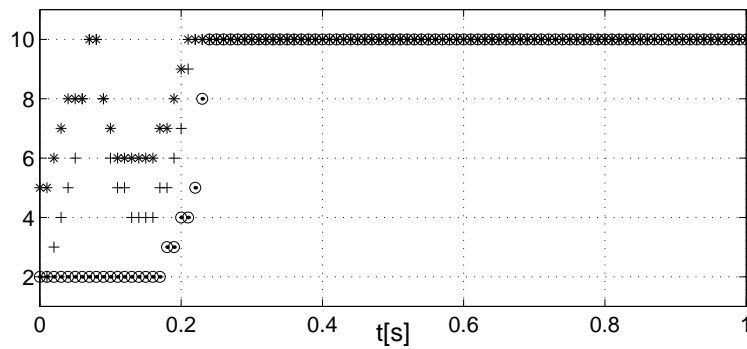


Figure 5: The results of simulation 1. Values of the index  $i$  of the linear regions  $\Gamma_{\rho_i,1}$  (o),  $\Gamma_{\rho_i,2}$  (.),  $\Gamma_{\rho_i,3}$  (+) and  $\Gamma_{\rho_i,4}$  (\*).

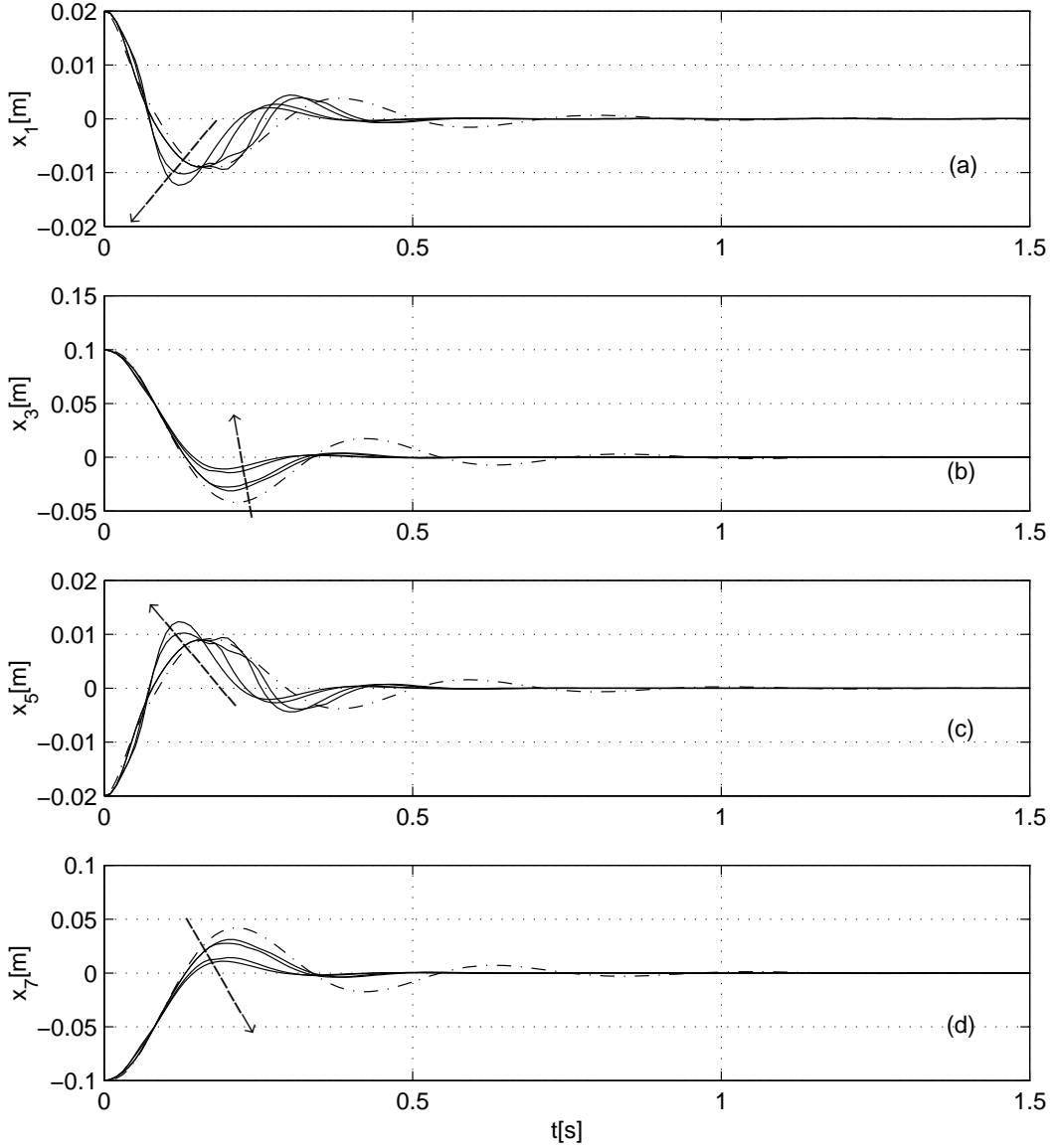


Figure 6: *The results of simulation 2. The arrow denotes the verse of increasing  $u_{\max}$ . (a) Evolution of  $x_1$  in the case of a passive suspension system (dotted) and  $x_{1,OGS}$  for  $u_{\max} = 400, 700, 1000, 1300N$  (continuous). (b) Evolution of  $x_3$  in the case of a passive suspension system (dotted) and  $x_{3,OGS}$  for  $u_{\max} = 400, 700, 1000, 1300N$  (continuous). (c) Evolution of  $x_5$  in the case of a passive suspension system (dotted) and  $x_{5,OGS}$  for  $u_{\max} = 400, 700, 1000, 1300N$  (continuous). (d) Evolution of  $x_7$  in the case of a passive suspension system (dotted) and  $x_{7,OGS}$  for  $u_{\max} = 400, 700, 1000, 1300N$  (continuous).*

## 5.2 Simulation 2

In the second simulation we compare the performances of a completely passive suspension system with tandem active-passive suspension systems characterized by different values of the constraint on the active forces.

The numerical values of the parameters relative to the completely passive suspension are the same as those of the passive part in the tandem suspension system. We assume the same value of the initial state as those in the previous subsection.

The main results of the comparison are reported in figure 6 where we can observe the variations of the system evolution in presence of actuators of increasing size. We have considered four different values for  $u_{max}$ : 400, 700, 1000, 1300N whose increasing value is denoted by an arrow. Figures 6.a and 6.c compares the deformation of the left and right tire, respectively, for the completely passive suspension with those of the tandem active-passive suspensions. In these figures we can note that as  $u_{max}$  is increased the unsprung mass reaches sooner the equilibrium state albeit with a greater overshoot in the first time instants. Figures 6.b and 6.d compare the deformation of the left and right suspension respectively, for the completely passive system, with those of the tandem active-passive suspensions. In these figures we observe that as  $u_{max}$  is increased the sprung mass reaches sooner the equilibrium state with decreasing overshoots. We can also observe that the lessening of the suspensions deformations are always less significant as  $u_{max}$  exceeds 700N. Therefore, we conclude that it is possible to guarantee good performances even with relatively small size actuators which, furthermore, limit the overshoots of the tires deformations.

## 5.3 Simulation 3

In this subsection we introduce an external disturbance given by the road profile.

Let us first discuss how its presence modifies the state space equation (8). Let  $w_L(t)$  and  $w_R(t)$  reported in figures 1–2, be the absolute vertical velocities of the points of contact with the road of the left and right tire respectively. Such velocities are caused by the uneven road profile and can be white noise signals, which is equivalent to saying that any longitudinal road profile can be represented by an integrated white noise [6, 9, 16]. Here, the road roughness characteristics are expressed by a signal whose PSD distribution function is [9]:

$$\Psi(\omega) = \frac{cV}{\omega^2 + \alpha^2 V^2} \quad (19)$$

where  $c = (\sigma^2/\pi)\alpha$ . Here  $\sigma^2$  denotes the road roughness variance and  $V$  the vehicle speed, whereas the coefficients  $c$  and  $\alpha$  depend on the type of road surface. The product is the power spectrum of the white noise. The signal  $x_{0,L}(t)$ , whose PSD is given by (19), may be obtained as the output of a linear filter expressed by the differential equation

$$\dot{x}_{0,L}(t) = -\alpha V x_{0,L}(t) + w_L(t) \quad (20)$$

where the subscript  $L$  stands for left. The same holds for the right disturbance.

By taking into account the above disturbances, state equation (8) can be rewritten as

$$\dot{\mathbf{x}}(t) = \mathbf{A}\mathbf{x}(t) + \mathbf{B}\mathbf{u}(t) + \mathbf{L}\mathbf{w}(t) \quad (21)$$

where  $\mathbf{w} = [w_L(t) \ w_R(t)]^T$  is the disturbance vector and  $\mathbf{L} \in \mathbb{R}^{8 \times 2}$  is defined as:

$$\mathbf{L} = \begin{bmatrix} -1 & f_t/M_1 & 0 & 0 & 0 & 0 & 0 & 0 \\ 0 & 0 & 0 & 0 & -1 & f_t/M_1 & 0 & 0 \end{bmatrix}^T.$$

In this simulation test we assume that the disturbance acting on the system is caused by a very rough road profile. Crosby and Karnopp [5] gave the power spectral density for such an input disturbance. We were able [6] to obtain a similar power spectral density by choosing in equation (19) the following parameter values:  $\alpha = 0.2 \text{ m}^{-1}$ ,  $\sigma^2 = 0.1 \text{ m}^2$  and  $V = 20 \text{ m/s}$ . Furthermore, we assume  $u_{max} = 500 \text{ N}$  and a null initial state.

The results of simulation 3 are shown in figures 7–8. Figure 7.a (7.b) shows the left (right) road profile along with the left (right) wheel and left (right) sprung mass displacement. It is possible to observe that the suspension filters the high frequencies smoothing the movement of the sprung mass. Figure 7.c shows the active forces  $u_1$  and  $u_2$ , while the total forces  $u_{T1}$  and  $u_{T2}$  are reported in figure 7.d. Figure 8 is similar to figure 5 relative to Simulation 1. Figure 8.a shows the values of the index  $i$  of the linear regions  $\Gamma_{\varrho_i,1}$  and  $\Gamma_{\varrho_i,3}$ , while the values of  $\Gamma_{\varrho_i,2}$  and  $\Gamma_{\varrho_i,4}$  are reported in figure 8.b.

## 6 Conclusions

In this work we have presented a design methodology for tandem active-passive suspension systems. More precisely, we have dealt with a half-car vehicle model. The design procedure is based on the minimization of a quadratic performance index that penalizes the tires and the suspensions deformations. We also required that the total forces applied between wheel and body and that the fraction of the forces generated by the actuators never exceed given bounds.

The constraint on the actuator forces can be used to dimension the actuators, so that it is required to provide only a fraction of the total forces generated by the suspension systems.

The constraint on the total forces bounds the acceleration on the sprung masses so as to ensure the comfort of passengers and to reduce the risk of loss of contact between wheels and road. Simulations showed that these constraints are active only when the system state is far from the origin.

Note that the proposed solution to this design problem has been obtained by a modification of a procedure firstly presented by Yoshida *et al.*. The solution takes the form of a state feedback law that switches between a finite set of constant gains.

The results of same numerical simulations for a half-car vehicle model have also been presented.

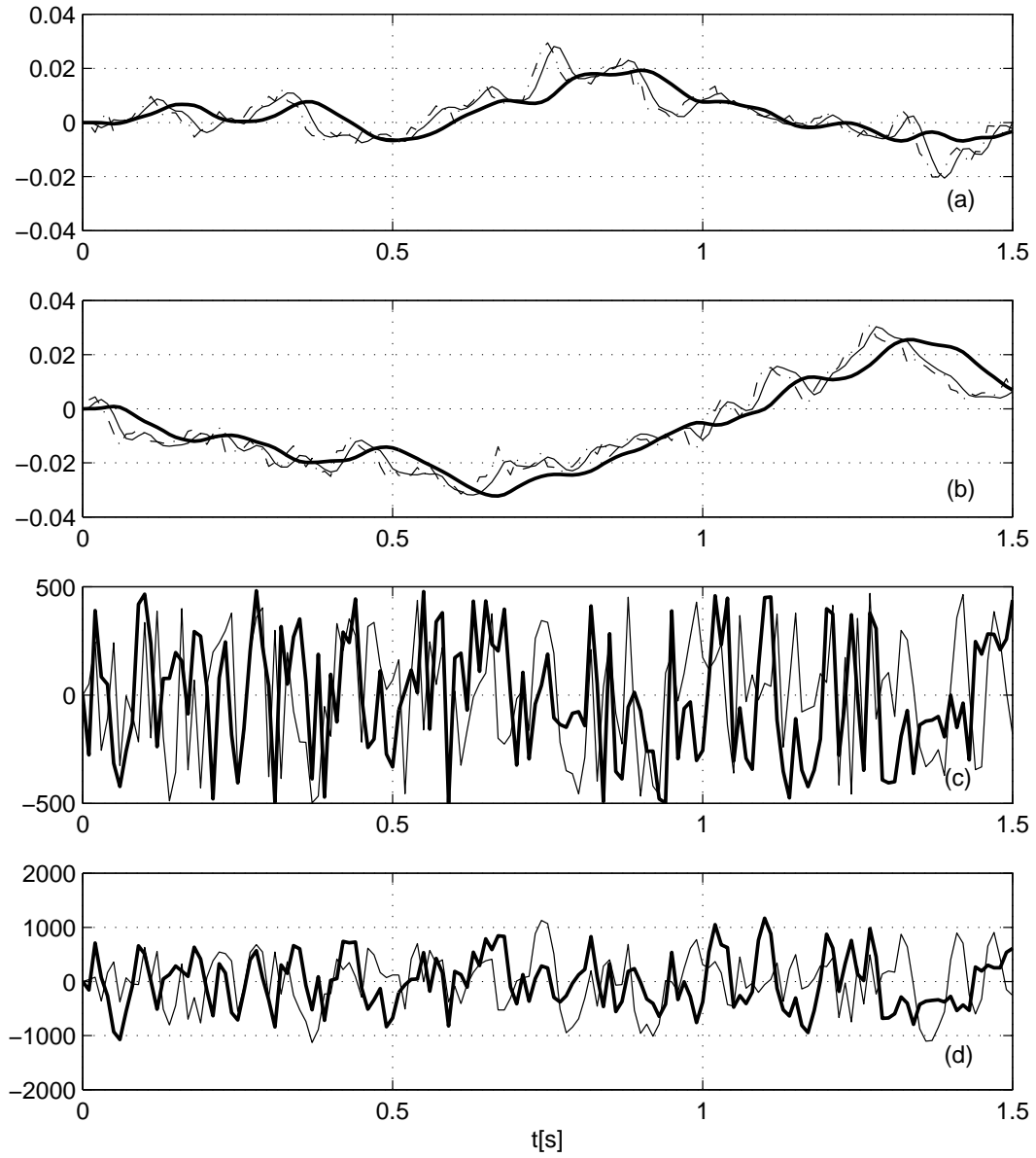


Figure 7: The results of simulation 3. (a) Evolution of  $x_{0,L}$  (dotted) and  $x_1+x_{0,L}$  (thin) and  $x_1+x_3+x_{0,L}$  (thick). (b) Evolution of  $x_{0,R}$  (dotted) and  $x_5+x_{0,R}$  (thin) and  $x_5+x_7+x_{0,R}$  (thick). (c) Evolution of  $u_1$  (thin) and  $u_2$  (thick). (d) Evolution of  $u_{T1}$  (thin) and  $u_{T2}$  (thick).

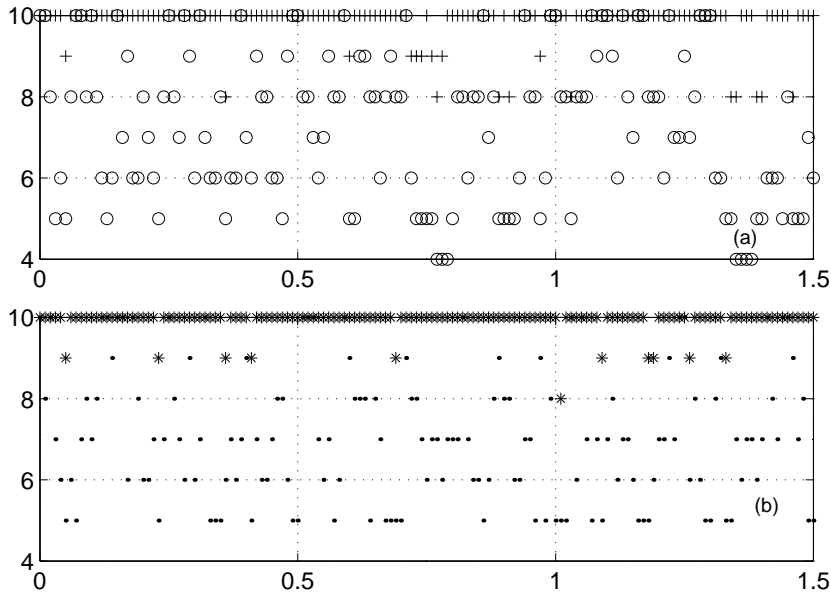


Figure 8: The results of simulation 3. (a) Values of the index  $i$  of the linear regions  $\Gamma_{\varrho_i,1}$  ( $\circ$ ) and  $\Gamma_{\varrho_i,3}$  ( $+$ ). (b) Values of the index  $i$  of the linear regions  $\Gamma_{\varrho_i,2}$  ( $\cdot$ ) and  $\Gamma_{\varrho_i,4}$  ( $*$ ).

An interesting extension to this work, and to the OGS procedure in general, would be that of analyzing the influence of an asymptotic state observer on the closed loop system. In particular, it would be important to investigate what may happen if a wrong region is selected and provide a bound on the maximum acceptable initial state error.

## Appendix

The optimal control input  $\mathbf{u}$  for system (2) that minimizes (3) can be determined as follows [20].

**Algorithm 3.** *Perfect Optimal Controller (POC).*

*Off-line phase*

1. Choose a large value for  $\varrho$  such that the second term in the performance index (5) is practically negligible. We denote this gain factor as  $\varrho_\infty$ .
2. Determine the corresponding gain vector  $\mathbf{k}_{\varrho_\infty}$  by solving an LQR problem with performance index of the form (5).
3. Construct the corresponding matrices  $\mathbf{Z}_{\varrho_\infty,j}$ ,  $j = 1, \dots, p$ .

*On-line phase*

1. Let  $k := 1$ .

2. Given the initial state  $\mathbf{x}_0$ , use the control law where the first  $k$ 's controls  $\mathbf{u}(i)$ ,  $0 \leq i \leq k-1$  satisfy the given  $p$  constraints of the form (3.b), while the rest are given by

$$\mathbf{u}(i) = -\mathbf{k}_\infty \mathbf{x}(i), \quad i \geq k.$$

Then the performance index (5) becomes a quadratic function of  $\mathbf{u}(i)$ ,  $0 \leq i \leq k-1$  and its minimizing argument can be found solving a quadratic programming problem.

3. If  $\mathbf{x}(k) \in \bigcap_{j=1}^p \Gamma_{\rho_\infty, j}$  then the perfect optimal control law becomes:

$$\mathbf{u} = \begin{cases} \mathbf{u}(i), & 0 \leq i < k \\ -\mathbf{k}_{\rho_\infty} \mathbf{x}(i), & i \geq k. \end{cases}$$

If not,  $k := k + 1$  and return to Step 2. ■

## Acknowledgements

The authors are grateful to the anonymous referee that suggested how the reduced matrix  $\tilde{\mathbf{Z}}_\rho$  could be constructed in the multi-constraint case (Section 2.2).

## References

- [1] K.C. Cheok, N.K. Loh, H.D. McGree, T.F. Petit, "Optimal model following suspension with microcomputerized damping," *IEEE Trans. on Industrial Electronics*, Vol. 32, No. 4, November 1985.
- [2] G. Corrigan, A. Giua, G. Usai, "An  $H_2$  formulation for the desing of a passive vibration-isolation system for cars," *Vehicle System Dynamics*, Vol. 26, pp. 381–393, 1996.
- [3] G. Corrigan, S. Sanna, G. Usai, "An optimal tandem active-passive suspension for road vehicles with minimum power consumption," *IEEE Trans. on Industrial Electronics*, Vol. 38, No. 3, pp. 210–216, 1991.
- [4] G. Corrigan, V. Presicci, S. Sanna, G. Usai, "Minimum energy optimal suspension for road vehicles," *Proc. Canadian Conference and Exhibition on Industrial Automation*, pp. 26.5–26.12, June 1992.
- [5] M.J. Crosby, D.C. Karnopp, "The active damper: a new concept in shock and vibration control," *43rd Shock and Vibration Bulletin*, June 1973.
- [6] A. Giua, C. Seatzu, G. Usai, "Semiactive suspension design with an Optimal Gain Switching target," *Vehicle System Dinamics*, Vo. 31, N. 4, pp. 213–232, April 1999.
- [7] E. Göring, E.C. von Glasner, R. Povel, P. Schützner, "Intelligent suspension systems for commercial vehicles," *Proc. Int. Cong. MV2, Active Control in Mechanical Engineering* (Lyon, France), pp. 1–12, June 1993.

- [8] M. Grima, C. Renou, “Modelization of semiactive suspensions,” *Proc. Int. Cong. MV2, Active Control in Mechanical Engineering* (Lyon, France), Vol. 1, June 1993, (in French).
- [9] A. Hac, “Suspension optimisation of a 2-DOF vehicle model using a stochastic optimal control technique,” *Journal of Sound and Vibration*, Vol. 100, No. 3, pp. 343–357, 1985.
- [10] D. Hrovat, “Survey of Advanced Suspension Developements and Related Optimal Control Applications,” *Automatica*, Vol. 33, No. 10, pp. 1781–1817, 1997.
- [11] E.J. Krasnicki, “Comparison of analytical and experimental results for a semiactive vibration isolator,” *Journal of Sound and Vibration*, pp. 69–76, September 1980.
- [12] H. Kwakernaak, R. Sivan, *Linear Optimal Control Systems*, Wiley Interscience (New York), 1972.
- [13] K. Ogata, *Discrete-time control systems*, Prentice Hall International editions, 1972.
- [14] V. Roberti, B. Ouyahia, A. Devallet, “Oleopneumatic suspension with preview semi-active control law,” *Proc. Int. Cong. MV2, Active Control in Mechanical Engineering* (Lyon, France), Vol. 1, June 1993.
- [15] J.S. Shamma, “Analysis and Design of Gain Scheduled Control systems” *Doctoral Thesis*, Laboratory for information and Decision Systems, Massachusetts Institute of Technology, Cambridge, Massachusetts, May, 1988.
- [16] A.G. Thompson, “An active suspension with optimal linear state feedback,” *Vehicle System Dynamics*, Vol. 5, pp. 187–203, 1976.
- [17] W.M. Wonham, C.D. Johnson, “Optimal bang-bang control with quadratic performance index,” *Trans. ASME Journal of Basic Engineering*, Vol. 86, pp. 107–115, March 1964.
- [18] K. Yoshida, Y. Nishimura, Y. Yonezawa, “Variable gain feedback for linear sampled-data systems with bounded control,” *Control Theory and Advanced Technology*, Vol. 2, No. 2, pp. 313–323, June 1986.
- [19] K. Yoshida, H. Kawabe, Y. Nishimura, M. Oya, “A simple LP formulation of the continuous-time positive invariance condition and its application to the constrained regulator problem,” *Proc. of the 35th Conf. on Dec. and Control* (Kobe, Japan), December 1996.
- [20] K. Yoshida, *Personal Communication*, 1997.